Research Article | Vol. 3, No. 8 / 15 August 2020 / OSA Continuum 2086


# Adjustable amplitude-phase hybrid gratings: intensity-sharing management between diffraction orders

SAIFOLLAH RASOULI[1,2,*] AND POURIA AMIRI[1]

[1] Department of Physics, Institute for Advanced Studies in Basic Sciences (IASBS), Zanjan 45137-66731, Iran
[2] Optics Research Center, Institute for Advanced Studies in Basic Sciences (IASBS), Zanjan 45137-66731, Iran
[*] rasouli@iasbs.ac.ir

**Abstract:** In this work, we propose a method for designing an adjustable amplitude-phase hybrid grating in which by relative lateral shearing of its amplitude and phase parts, the intensity share between different diffraction orders can be controlled. The method is based on superimposing two pure-amplitude and pure-phase gratings with sinusoidal or binary profiles having the same periods and lines' orientations. It is shown that, in the diffraction of a Gaussian beam from such hybrid gratings, the intensity share of each of the diffraction orders is related to the shear value and the amplitude of the transmission functions of the superimposed pure-amplitude and pure-phase gratings. For instance, when both of the amplitude and phase profiles are sinusoidal and the shear value between them is a quarter of the period, for given values of the transmissions amplitudes of the profiles, all positive (or negative) diffraction orders are removed. We also show that, by changing the values of the transmission's amplitudes, the intensity share for the higher orders can be increased. This kind of grating might find application in optical switching and in devices requiring power sharing between different channels such as in beam-steering devices, in optical interconnects, and in optical fiber communication.



## 1. Introduction

The diffraction grating is one of the most famous diffraction elements, long and thoroughly investigated. Gratings play important roles in the operation of many optical equipment. The main components in the spectroscopy [1] and moiré deflectometry [2] are the gratings. Gratings are also widely used in the metrology, shearing interferometry [3–5], vibration and displacement transducers [2,6], lithography [7–9], wave-front sensing [10], optical alignment technique, strain and stress analysis, and moiré topography. The diffraction gratings are also used as beam splitters [11–13], as chromatic dispersive elements [14–16], for (de)multiplexing optical signal in communications [17,18], for laser processing [19,20], for optical vortices characterizing and multiplying [21–23], and other.

The physics of the diffraction from gratings is an interesting topic, it has attracted much attention and many studies allocated to it. In the diffraction of a plane wave from a conventional grating that has equidistant parallel lines, the beam is split and diffracted into several beams travelling in different directions. The diffracted beams are known as diffraction orders. For such gratings, the intensities of diffraction orders decrease with increasing the number of order of diffraction. A way to increase the optical power in a higher diffraction order is the use of gratings with a special form of transmission or reflection profile. In a blazed-grating [24], it has parallel rulings with a sawtooth profile, maximum optical power is concentrated in a given diffraction order while the residual power in the other orders, particularly in the zeroth, is minimized.

#399092 https://doi.org/10.1364/OSAC.399092
Journal © 2020 Received 1 Jun 2020; revised 9 Jul 2020; accepted 9 Jul 2020; published 31 Jul 2020

OSA CONTINUUM

We recently constructed a new type of gratings by adding an azimuthal periodic dependency to the argument of the transmission function of a linear phase grating that has a sinusoidal profile and we named them azimuthally-modified linear phase gratings (AMLPGs) [25]. In the diffraction of a plane wave from an AMLPG, it observed that the different diffraction orders are similar radial carpet beams having some small differences. Unlike the conventional gratings, for an AMLPG the intensity of a given higher order diffracted beam can be higher than the intensities of the lower order beams. It was shown that the intensity sharing among different diffracted beams can be adjusted by the value of the phase amplitude of the host linear grating.

Now, in this work we introduce a method for designing an adjustable amplitude-phase hybrid grating in which by a relative lateral shearing of its amplitude and phase parts, the intensity share between different diffraction orders can be controlled. The method is based on superimposing two pure-amplitude and pure-phase gratings with sinusoidal or binary profiles having the same periods and lines orientations. It is shown that, in the diffraction of a Gaussian beam from such hybrid grating, the intensity sharing between the diffraction orders is related to the shear value, and the amplitude of the transmission functions of the superimposed pure-amplitude and pure-phase gratings. This kind of gratings might find wide applications in many areas of optics such as optical switches.

It needs to mention that, many methods and devices were proposed for beam-steering and beam-controlling such as construction of prism grating with polymer stabilized nematic liquid crystal [26], optically-tunable beam steering grating with the use of azobenzene doped cholesteric liquid crystal [27], large-angle and high-efficiency tunable phase grating with the use of fringe field switching liquid crystal [28], image-induced blazed gratings for high speed all-optical beam controlling [29], and diffractive transmission grating was tuned by dielectric elastomer actuator [30]. More or less, the experimental methods presented in the above references can be used in the implementation of our proposed method for generation of adjustable amplitude-phase hybrid gratings. However, we discuss about some possible experimental setups to implement the proposed method.

## 2. Governing equations and simulations

Here, we introduce adjustable amplitude-phase hybrid gratings and present the governing equations of the diffraction of a Gaussian beam from such gratings. We call a grating with the following complex transmission function as an adjustable amplitude-phase hybrid grating:

$$t(x,y) = \frac{1}{2}\left(1 + V_a cos[\frac{2\pi}{d}x]\right) \exp\left(iV_p cos[\frac{2\pi}{d}(x-\Delta x)]\right). \tag{1}$$

Here, we considered sinusoidal profiles for both amplitude and phase parts of the grating with the same period $d$. $V_a$ shows the visibility of the amplitude part where $0<V_a<1$, similarly $V_p$ denotes the maximum phase variation on the phase part in which $-\pi<V_p<+\pi$, and $\Delta x$ indicates a given lateral shear between the amplitude and phase parts of the grating in which $0<\Delta x<d$. Hereafter, we call the the first and second terms in Eq. (1) as the pure-amplitude and pure-phase parts of the hybrid grating, respectively. One can consider a binary profile for one or both of the amplitude and phase parts of the hybrid grating by replacing the $\cos(\cdots)$ terms with the corresponding sign values $sgn[\cos(\cdots)]$ in Eq. (1), where $sgn$ is the sign function.

In the Cartesian coordinates system, the amplitude of a Gaussian beam over the x-y plane can be written in the following form:

$$u(x,y;-0) = \exp(-\frac{x^2+y^2}{w^2}), \tag{2}$$

OSA CONTINUUM

where $w$ shows the radius parameter of the beam. After passing the beam through a hybrid grating, the light beam complex amplitude immediately after the grating is

$$u(x, y; +0) = t(x, y)u(x, y; -0), \tag{3}$$

where $-0$ and $+0$ signify immediately before and after the grating, respectively. Therefore, we consider $u(x, y; +0)$ as the complex amplitude of the light beam at $z = 0$.

Figure 1 shows the intensity and phase profiles of a Gaussian beam with $w = 0.5$ mm, the amplitude and phase profiles of different hybrid gratings having sinusoidal or binary profile with the same period, and $V_a = 1$ and $V_p = \pi$, and the corresponding intensity and phase profiles of the transmitted beam immediately after the gratings.

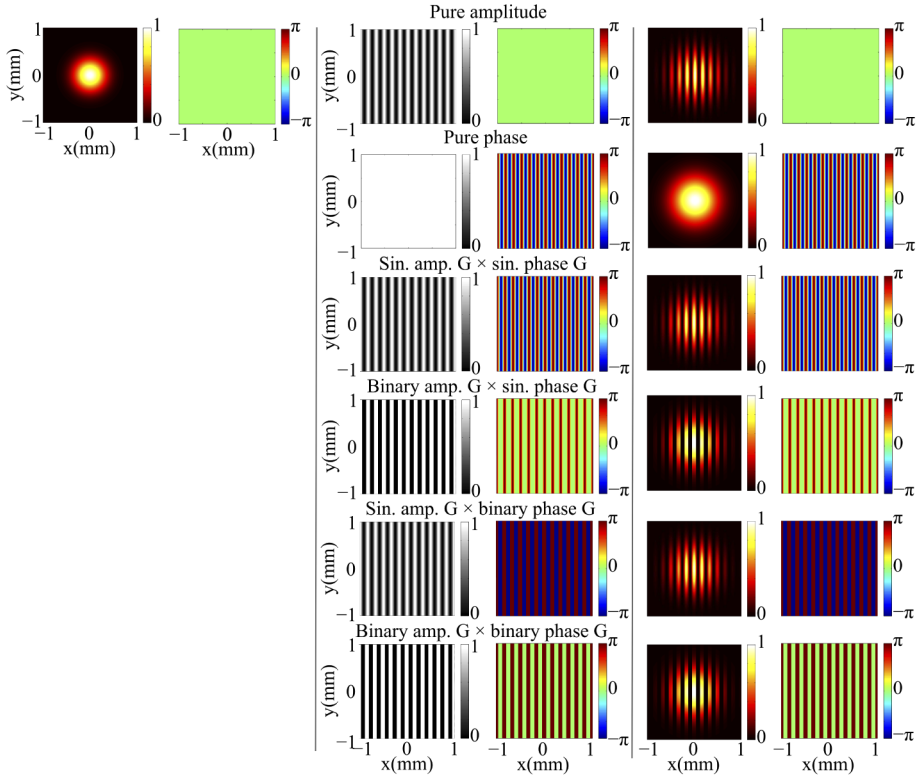


**Fig. 1.** From the left to right columns, the intensity and phase profiles of a Gaussian beam with $w = 0.5$ mm, the amplitude and phase profiles of amplitude-phase hybrid gratings having sinusoidal/binary profile with $d = 0.16$ mm, $V_a = 1$, and $V_p = \pi$, and the corresponding intensity and phase profiles of the transmitted beam immediately after the gratings. For all cases $\Delta x = 0$

The diffracted complex amplitude after a propagation distance of $z$, $u(x', y'; z)$, can be calculated using the Fresnel integral as

$$u(x', y'; z) = \frac{e^{ikz}}{iz\lambda} \int_{-\infty}^{+\infty} \int_{-\infty}^{+\infty} u(x, y; +0) \exp\left(i\alpha[(x - x')^2 + (y - y')^2]\right) dx\, dy, \tag{4}$$

where $\alpha = \frac{\pi}{z\lambda}$, in which $\lambda$ is the wavelength of the light beam and $k = \frac{2\pi}{\lambda}$ is the wave-number, and using Eqs. (2) and (3), and considering binary profiles for both amplitude and phase parts of

OSA CONTINUUM

the hybrid grating we have.

$$u(x, y; +0) = \frac{1}{2} \exp\left(\frac{x^2 + y^2}{w^2}\right)\left(1 + V_a \left|cos[\frac{2\pi}{d}x]\right|\right) \exp\left(iV_p \left|cos[\frac{2\pi}{d}(x - \Delta x)]\right|\right). \quad (5)$$

Three other cases having sinusoidal profiles can be consider by removing one or both of the sign functions (saving the cosine functions) in the first and/or second terms in Eq. (5).

Now, using Eq. (4) and with the aid of transfer function of the free space, we simulate the intensity and phase profiles of the diffracted pattern after different propagation distances. Figure 2 shows diffraction patterns of a Gaussian beam from different amplitude-phase hybrid gratings formed in the superimposition of two pure-amplitude and pure-phase gratings having sinusoidal/binary profile with $V_a = 1$, $V_p = \pi$, and the same period, for different lateral shear values of the pure-amplitude and pure-phase parts, $\Delta x$, at a propagation distance $z = 1.2$ m. The background Visualization 1, Visualization 2, Visualization 3, and Visualization 4 present evolution of the diffracted patterns were calculated at different propagation distances. One can see that, for the case of first column, second row, almost all of the positive diffraction orders are removed and -2 order has the maximum value of intensity. In fact in this case, the diffracting object acts as a binarized blazed-grating [31], Besides, it should be noted that variations of the fill factor of a grating makes it possible to control the intensity distribution in various orders not only for linear, but also for circular gratings [32,33].

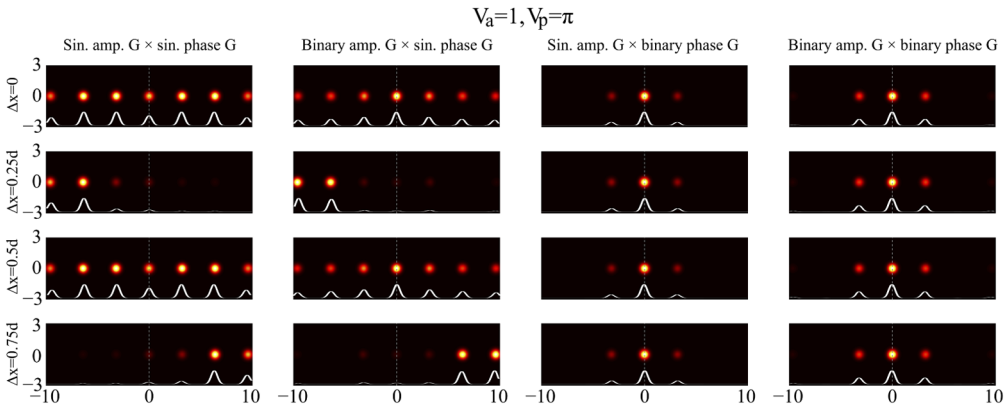


**Fig. 2.** Diffracted patterns of a Gaussian beam with $w = 0.5$ mm and $\lambda = 532$ nm from different amplitude-phase hybrid gratings formed in the superimposition of two pure-amplitude and pure-phase gratings having sinusoidal/binary profile with $d = 0.16$ mm, $V_a = 1$, and $V_p = \pi$, for different lateral shear values of the pure-amplitude and pure-phase parts, $\Delta x$, at a propagation distance $Z = 1.2$ m (See Visualization 1, Visualization 2, Visualization 3, and Visualization 4).

Figure 3 shows the same diffraction patterns (and links the same visualizations) of Fig. 2 with the same parameters except $V_a = 1$ and $V_p = 1$. As it is seen in first column, second row, all of the positive diffraction orders are removed and -1 order has the maximum value of intensity. It is worth mentioning that, a similar asymmetric diffraction behavior was previously reported for prism grating created using polymer stabilized nematic liquid crystal [26].

In Fig. 4, the same diffraction patterns of Fig. 2 with the same parameters except $V_a = 0.5$ and $V_p = 0.5\pi$ are shown and the corresponding visualizations are also linked. Here, at the third column ±1 diffraction orders have the maximum values of intensity even more than the DC term (the zero order).

In Fig. 5, the same visualizations and diffraction patterns of Fig. 2 with the same parameters except $V_a = 1$ and $V_p = 0.25\pi$ are linked and shown, respectively. Here, at the first column,

OSA CONTINUUM

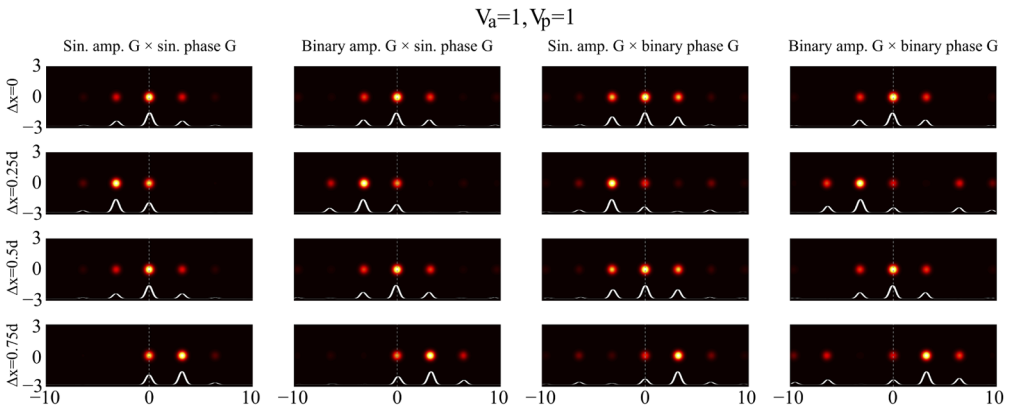


**Fig. 3.** The same diffraction pattern of Fig. 2 with the same parameters except here $V_a = 1$ and $V_p = 1$ (See also Visualization 5, Visualization 6, Visualization 7, and Visualization 8).

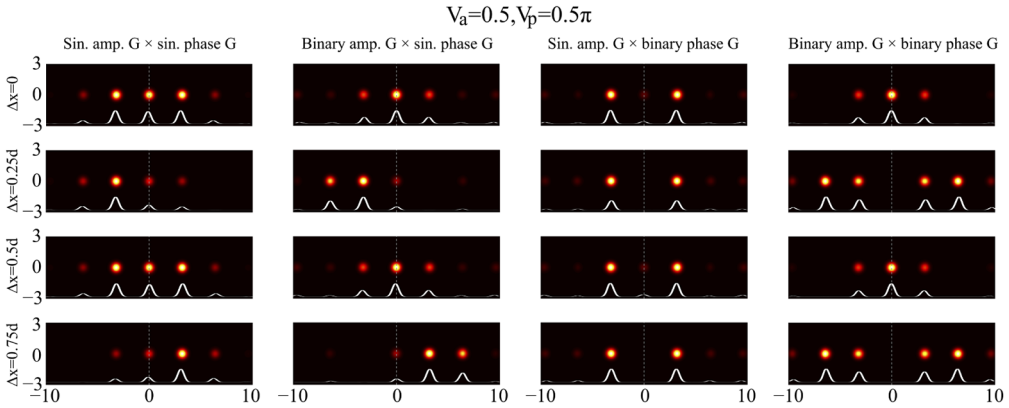


**Fig. 4.** The same diffraction pattern of Fig. 2 with the same parameters except $V_a = 0.5$ and $V_p = 0.5\pi$. See also Visualization 9, Visualization 10, Visualization 11, and Visualization 12.

second and last rows, the zero and one of the first diffraction orders have the same and maximum values of intensities.

Figure 6 presents the same diffraction patterns and visualizations of Fig. 2 when $V_a = 0.25$, $V_p = \pi$, and other parameters are the same. Here, at the second column, second and last rows, two neighbor second and third diffraction orders have the same and maximum values of intensities. It is also seen that, in the first column, first and third rows, the ±2 diffraction orders have the same and maximum values of intensities.

Figure 7 shows the ratios of the mean values of the intensities over the first order diffracted pattern ($I_{+1}$) to the mean value of the incident beam intensity ($I_0^-$) and the transmitted beam intensity ($I_0^+$) for the cases were presented in Figs. 2 and 3. It is seen that, for the shear value $\Delta x = 0.75d$ the intensity share for the first diffraction order is maximum, and for the case of sinusoidal amplitude and phase profiles with $V_a = 1$ and $V_p = 1$ more than half of the transmitted energy flows to +1 diffraction order. In that case, when $\Delta x = 0.25d$, the intensity of the +1 diffraction order is zero.

In Fig. 8, plots show the ratios of the mean values of the intensities over the different diffracted orders ($I_{+i}$) to the mean value of the incident beam intensity ($I_0^-$) as a function of shear value $\Delta x$, for the cases were presented in Figs. 2–6. One can consider some behaviors of the intensity

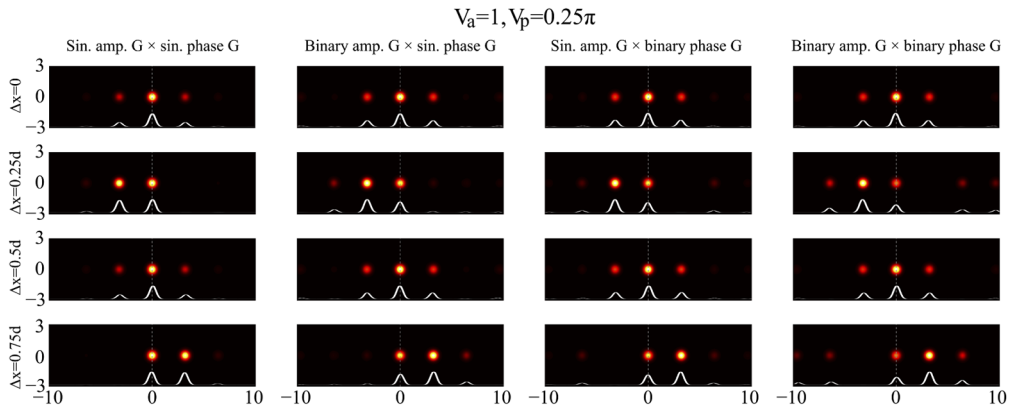


**Fig. 5.** The same diffraction pattern of Fig. 2 with the same parameters except here $V_a = 1$ and $V_p = 0.25\pi$. See also Visualization 13, Visualization 14, Visualization 15, and Visualization 16.

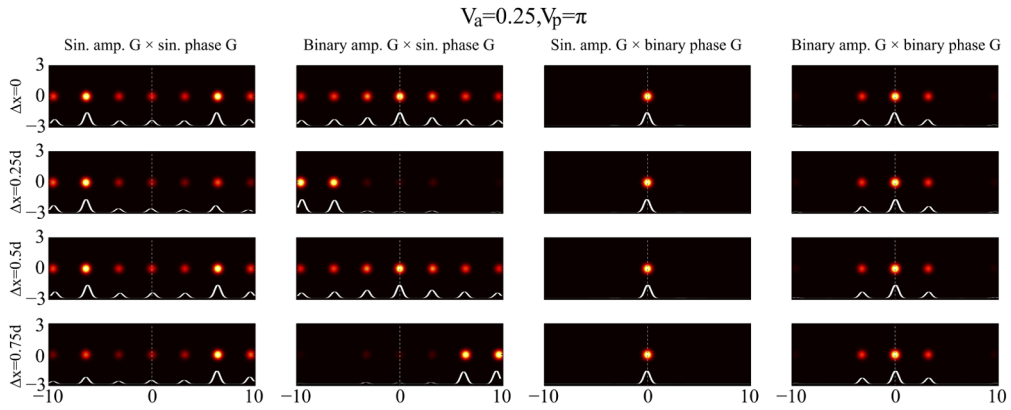


**Fig. 6.** The same diffraction pattern of Fig. 2 with the same parameters except here $V_a = 0.25$ and $V_p = \pi$. See also Visualization 17, Visualization 18, Visualization 19, andVisualization 20.

sharing between different diffraction orders using these plots. For instance, let us consider the case presented in the first column, last row. It is seen that, the total intensities of two ±2 diffraction orders are constant in which by changing the shear value, intensity share of one order decreases and for the other one it increases. This behavior can be used for gradually changing the energy share between two channels.

## 3. Additional discussion

It should be mentioned that, in the designing of diffractive optical elements, many methods were developed for coding the amplitude-phase distribution into only amplitude or only phase distribution [34–37]. The method proposed here involves not only a separate production of amplitude and phase gratings, but also their accurate displacement relative to each other by a fraction of the period. Therefore, it is needed to discuss about possible ways to implement experimentally the proposed method and how to align elements. To implement the idea presented here, some methods can be used in which to have two a pair of pure amplitude and phase gratings over each other and to displace them laterally. A possible way is to generate a pure amplitude

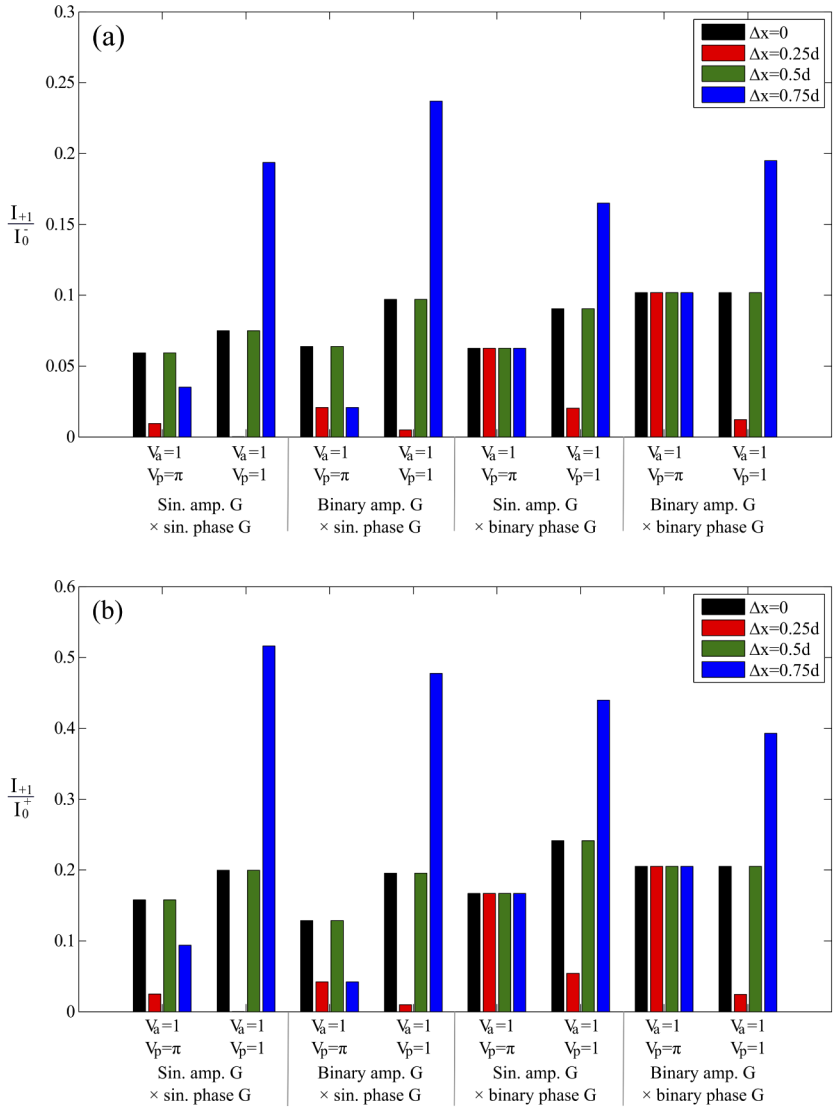


**Fig. 7.** The ratios of the mean values of the intensities over the first order diffracted pattern ($I_{+1}$) to the mean value of the (a) incident beam intensity ($I_0^-$) and (b) transmitted beam intensity ($I_0^+$) for the cases were presented in Figs. 2 and 3.

OSA CONTINUUM

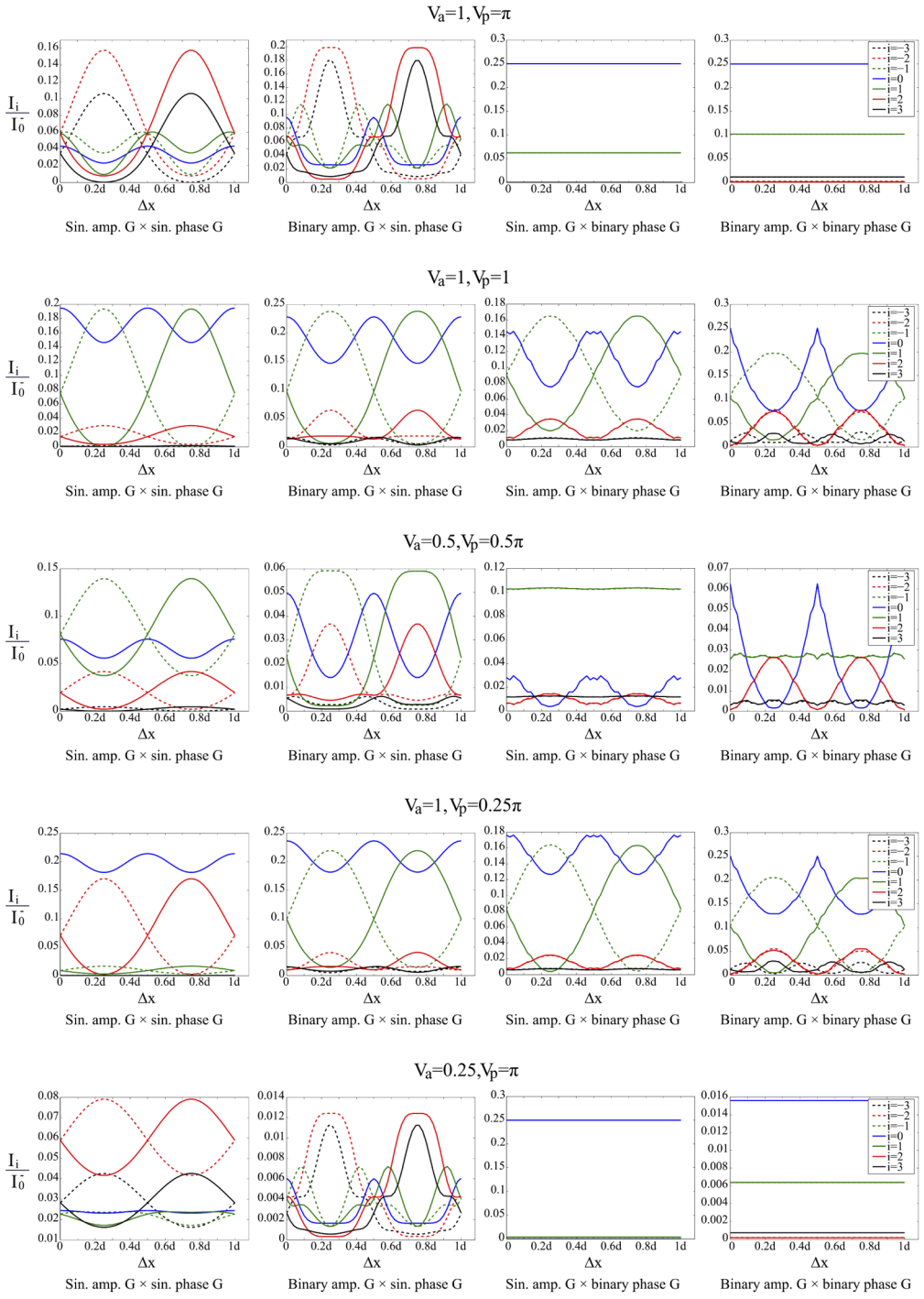


**Fig. 8.** Plots of the ratios of the mean values of the intensities over the different diffracted order ($I_{+i}$) to the mean value of the incident beam intensity ($I_0^-$) as a function of shear value $\Delta x$, for the cases were presented in Figs. 2–6.

OSA CONTINUUM

grating with the aid of Talbot images of an amplitude grating on a pure phase grating, in which the second one can be also generated with the aid of a professional SLM. Therefore, as amplitude and phase parts have a physical apart; lateral shearing of the them will be a very easy task. In addition, with the aid of Talbot images of two similar amplitude gratins when their planes and lines are parallel, one can produce 1D periodic intensity profile with a desired fringe sharpness (or fill factor) by implementing a lateral shift between these amplitude gratings. Now, in this scheme, the SLM generating the phase grating can be replaced just after the second amplitude grating or in one of its Talbot planes.

## 4. Conclusion

A novel method was introduced for designing an adjustable amplitude-phase hybrid grating to control the intensity share between different diffraction orders by lateral shearing of the amplitude and phase parts of the grating and by changing amplitudes of the transmission and phase profiles variations. It was shown that, when both superimposed structures have sinusoidal profiles and the shear value is quarter of the period, for given values of the transmissions amplitudes of the amplitude and phase parts, all positive (or negative) diffraction orders are removed, and by changing the values of the transmissions amplitudes the intensity share for the higher orders can be increased. The presented method is a good candidate for beam-steering and optical switching and might find many applications in optical fiber communication, optical interconnects, projection displays, and optical data storage.

## Funding

Iran National Science Foundation (98019152, 99003644).

## Disclosures

Authors declare no conflicts of interest.

## References

1. S. A. Akhmanov and S. Y. Nikitin, *Physical Optics* (Clarendon, 1997).
2. K. Patorski and M. Kujawinska, *Handbook of the Moiré Fringe Technique* (Elsevier, 1993).
3. S. Yokozeki and T. Suzuki, "Shearing interferometer using the grating as the beam splitter," Appl. Opt. **10**(7), 1575–1580 (1971).
4. S. Rasouli and M. Ghorbani, "Nonlinear refractive index measuring using a double-grating interferometer in pump-probe configuration and Fourier transform analysis," J. Opt. **14**(3), 035203 (2012).
5. S. Rasouli, F. Sakha, and M. Yeganeh, "Infinite-mode double-grating interferometer for investigating thermal-lens–acting fluid dynamics," Meas. Sci. Technol. **29**(8), 085201 (2018).
6. S. Rasouli and M. Shahmohammadi, "A portable and long-range displacement and vibration sensor that chases moving moiré fringes using the three-point intensity detection method," OSA Continuum **1**(3), 1012–1025 (2018).
7. D. Thomae, O. Sandfuchs, and R. Brunner, "Quantitative analysis of imperfect frequency multiplying in fractional Talbot planes and its effect on high-frequency-grating lithography," J. Opt. Soc. Am. A **31**(7), 1436–1444 (2014).
8. A. Naqavi, H. Peter Herzig, and M. Rossi, "High-contrast self-imaging with ordered optical elements," J. Opt. Soc. Am. B **33**(11), 2374–2382 (2016).
9. S. Rasouli and D. Hebri, "Contrast enhanced quarter-Talbot images," J. Opt. Soc. Am. A **34**(12), 2145–2156 (2017).
10. M. Dashti and S. Rasouli, "Measurement and statistical analysis of the wave-front distortions induced by atmospheric turbulence using two-channel moiré deflectometry," J. Opt. **14**(9), 095704 (2012).
11. B. Riccardo, C. Gabriella, and S. Massimo, "Diffractive variable beam splitter: optimal design," J. Opt. Soc. Am. A **17**(1), 63–67 (2000).
12. M. A. Golub, "Laser Beam Splitting by Diffractive Optics," Opt. Photonics News **15**(2), 36–41 (2004).
13. A. Porfirev, S. Khonina, Y. Azizian-Kalandaragh, and M. Kirilenko, "Efficient generation of arrays of closed-packed high-quality light rings," Photonics Nanostructures-Fundamentals Appl. **37**, 100736 (2019).
14. H. Dammann, "Color separation gratings," Appl. Opt. **17**(15), 2273–2279 (1978).
15. Y. Ogura, N. Shirai, J. Tanida, and Y. Ichioka, "Wavelength-multiplexing diffractive phase elements: design, fabrication, and performance evaluation," J. Opt. Soc. Am. A **18**(5), 1082–1092 (2001).
16. L. L. Doskolovich, N. L. Kazanskiy, S. N. Khonina, R. V. Skidanov, N. Heikkila, S. Siitonen, and J. Turunen, "Design and investigation of color separation diffraction gratings," Appl. Opt. **46**(15), 2825–2830 (2007).

OSA CONTINUUM


17. T. Lei, M. Zhang, Y. Li, P. Jia, G. N. Liu, X. Xu, Z. Li, C. Min, J. Lin, C. Yu, H. Niu, and X. Yuan, "Massive individual orbital angular momentum channels for multiplexing enabled by Dammann gratings," Light: Sci. Appl. **4**(3), e257 (2015).
18. A. Trichili, K. H. Park, M. Zghal, B. S. Ooi, and M. S. Alouini, "Communicating using spatial mode multiplexing: Potentials, challenges, and perspectives," IEEE Commun. Surv. & Tutorials **21**(4), 3175–3203 (2019).
19. S. Hasegawa, H. Ito, H. Toyoda, and Y. Hayasaki, "Massively parallel femtosecond laser processing," Opt. Express **24**(16), 18513–18524 (2016).
20. A. A. Kuchmizhak, A. P. Porfirev, S. A. Syubaev, P. A. Danilov, A. A. Ionin, O. B. Vitrik, Y. N. Kulchin, S. N. Khonina, and S. I. Kudryashov, "Multi-beam pulsed-laser patterning of plasmonic films using broadband diffractive optical elements," Opt. Lett. **42**(14), 2838–2841 (2017).
21. D. Hebri, S. Rasouli, and M. Yeganeh, "Intensity-based measuring of the topological charge alteration by the diffraction of vortex beams from amplitude sinusoidal radial gratings," J. Opt. Soc. Am. B **35**(4), 724–730 (2018).
22. P. Amiri, A. M. Dezfouli, and S. Rasouli, "Efficient characterization of optical vortices via diffraction from parabolic-line linear gratings," *J. Opt. Soc. Am. B*, under review (2020).
23. D. Hebri, S. Rasouli, and A. M. Dezfouli, "Theory of diffraction of vortex beams from structured apertures and generation of elegant elliptical vortex Hermite–Gaussian beams," J. Opt. Soc. Am. A **36**(5), 839–852 (2019).
24. W. Xu, W. Daniel, M. Richard, M. Paul, and P. Demetri, "Liquid-crystal blazed-grating beam deflector," Appl. Opt. **39**(35), 6545–6555 (2000).
25. S. Rasouli and A. M. Khazaei, "An azimuthally-modified linear phase grating: Generation of varied radial carpet beams over different diffraction orders with controlled intensity sharing among the generated beams," Sci. Rep. **9**(1), 12472 (2019).
26. H. Ren, Y. H. Fan, and S. T. Wu, "Prism grating using polymer stabilized nematic liquid crystal," Appl. Phys. Lett. **82**(19), 3168–3170 (2003).
27. H. Jau, T. Lin, R. Fung, S. Huang, J. H. Liu, and A. Y. G. Fuh, "Optically-tunable beam steering grating based on azobenzene doped cholesteric liquid crystal," Opt. Express **18**(16), 17498–17503 (2010).
28. D. Xu, G. Tan, and S. Wu, "Large-angle and high-efficiency tunable phase grating using fringe field switching liquid crystal," Opt. Express **23**(9), 12274–12285 (2015).
29. L. Zhao, W. Duan, and S. F. Yelin, "All-optical beam control with high speed using image-induced blazed gratings in coherent media," Phys. Rev. A **82**(1), 013809 (2010).
30. M. Aschwanden, M. Beck, and A. Stemmer, "Diffractive transmission grating tuned by dielectric elastomer actuator," IEEE Photonics Technol. Lett. **19**(14), 1090–1092 (2007).
31. S. N. Khonina and A. V. Ustinov, "Binary multi-order diffraction optical elements with variable fill factor for the formation and detection of optical vortices of arbitrary order," Appl. Opt. **58**(30), 8227–8236 (2019).
32. I. Amidror, "The Fourier-spectrum of circular sine and cosine gratings with arbitrary radial phases," Opt. Commun. **149**(1-3), 127–134 (1998).
33. A. V. Ustinov, A. P. Porfirev, and S. N. Khonina, "Effect of the fill factor of an annular diffraction grating on the energy distribution in the focal plane," J. Opt. Technol. **84**(9), 580–587 (2017).
34. J. P. Kirk and A. L. Jones, "Phase-Only Complex-Valued Spatial Filter," J. Opt. Soc. Am. **61**(8), 1023–1028 (1971).
35. O. Bryngdahl and F. Wyrowski, "Digital Holography–Computer-Generated Holograms," Prog. Opt. **61**, 1–86 (1990).
36. S. N. Khonina, V. V. Kotlyar, and V. A. Soifer, "Techniques for encoding composite diffractive optical elements," Proc. SPIE **5036**, 493–498 (2003).
37. O. Mendoza-Yero, G. Mãnguez-Vega, and J. Lancis, "Encoding complex fields by using a phase-only optical element," Opt. Lett. **39**(7), 1740–1743 (2014).